Journal of Industrial Aerodynamics, 2 (1977) 159—180

WIND PROTECTION BY MODEL FENCES IN A SIMULATED ATMOSPHERIC BOUNDARY LAYER

J.K. RAINE and D.C. STEVENSON

University of Canterbury, Christchurch (New Zealand)

(Received October 15, 1976; in revised form January 31, 1977)

Summary

A brief review of windbreak aerodynamics is presented and tests of model shelter fences in a simulated atmospheric boundary layer are described. Measurements of mean wind velocity, RMS velocity fluctuations and energy spectra for the streamwise velocity component were made in the lee of model fences of permeability 0%, 20%, 34% and 50%. Results of the tests are compared where possible with existing field and wind-tunnel data, with due regard for the uncertainty of hot-wire anemometer measurements in a bluff body wake. The turbulence measurements define the leeward flow regions which are dominated respectively by the bleed flow and by the displacement flow. For these two regions separate empirical relationships between mean velocity and turbulence intensity are given. In these tests the 20% permeable fence gave the best overall reduction in leeward mean velocity. However, in practice it may often be more cost-effective to build a relatively higher fence of greater permeability.

1. Introduction

Reports of windbreak performance frequently show disagreement between results of separate field tests of similar windbreaks. Generally quantitative agreement between full-scale and wind-tunnel model tests of windbreaks has also been mediocre. This is well illustrated by the comprehensive review of van Eimern et al. [1]. In addition there is a scarcity of turbulence measurements in the flow downstream from windbreaks and uncertainty as to the optimum permeability for a windbreak.

The tests of model shelter fences described here were carried out in a rigorously simulated neutrally stable atmospheric boundary layer [2]. The model flow had a 1/6-power-law mean velocity profile and turbulence structure characteristic of flow over a full-scale surface of roughness length z_0 = 50 mm. By carrying out mean-velocity and turbulence measurements it was intended to obtain a clearer picture of the leeward flow field and provide:

(i) greater justification for accepting results of model windbreak tests as indicative of full-scale performance;

(ii) a more quantitative relationship between mean velocity reduction and turbulent intensity downstream of shelter fences.

2. Windbreak aerodynamics — a review

2.1 Theoretical models — windbreak drag coefficients

The aerodynamic action of a windbreak is simple in principle. The windbreak exerts a drag force on the wind field, causing a nett loss of momentum in the incompressible airflow and thus a sheltering effect. As the permeability of a windbreak is reduced, the 'bleed flow' through the windbreak decreases and the drag force increases. This is accompanied by a greater upward deflection of the approach flow, and below a certain permeability, a region of large-scale separated flow in the lee of the windbreak. The more impermeable the barrier, the stronger appears to be the turbulent eddying in the separation zone and the steeper the return of the displacement flow to ground at its downstream reattachment point (see Fig.1). Kaiser [3] was probably the

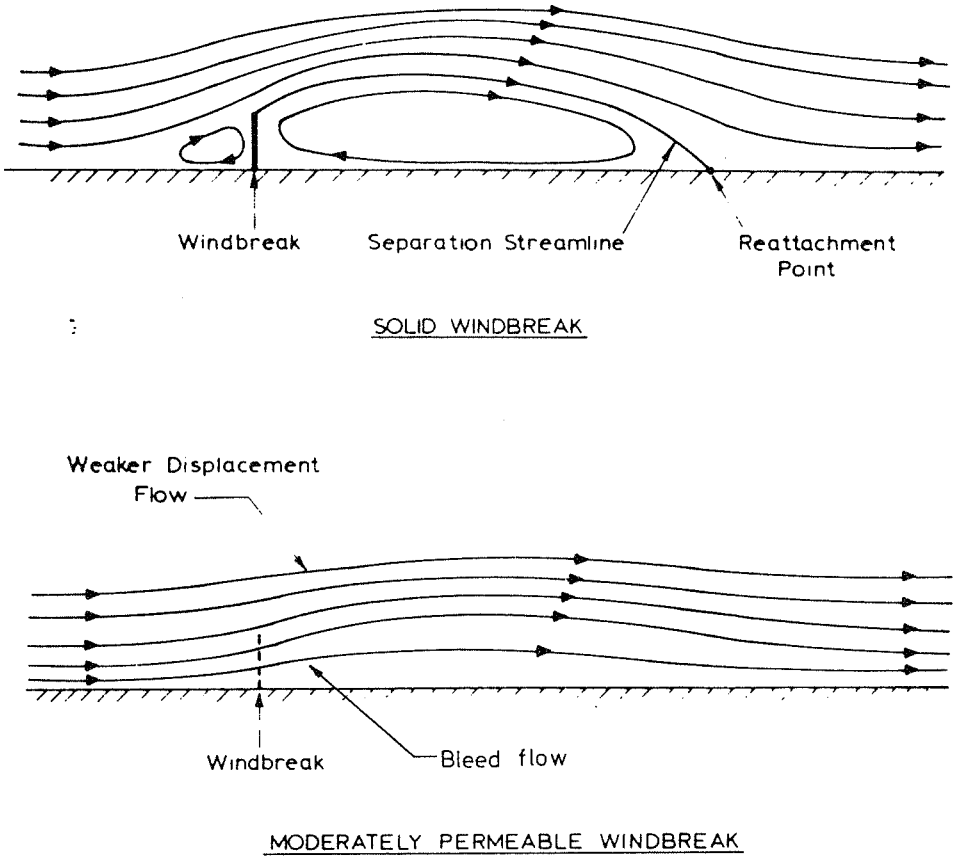

Fig.1. Streamline sketches of windbreak airflow.

first to make the distinction between 'mean wind reduction' and 'wind protection', pointing out that while a less permeable windbreak may cause a greater reduction in mean wind speed, the greater turbulence in its wake may make it less effective for overall wind protection than a more permeable one.

The lack of satisfactory analytical solutions to the Navier–Stokes equations in the highly turbulent flow in the region of a windbreak has led inevitably to a preference for empirical descriptions of windbreak airflow, based on field and wind-tunnel data. Kaiser [3] proposed a theoretical model for flow over a permeable barrier. The analysis treats first the top edge of the fence and later the whole fence surface as a momentum sink, and the three-dimensional diffusion equation is applied in analogy to diffusion of smoke downstream of a chimney. The theory gives a qualitative prediction of mean wind reduction in the lee of a windbreak but overestimates reduction of mean velocity in the sheltered zone. Seginer and Sagi [4] and Plate [5] have proposed theoretical models relating windbreak drag to the leeward mean velocity field. A control volume analysis of streamwise momentum loss in the flow over the barrier is used. Assumptions regarding mean velocity and shear distributions prevent these models from giving good quantatitive estimates of windbreak drag.

Experimental data from field and wind-tunnel tests show that windbreak drag increases with:

(i) decreasing permeability

(ii) an increase in the ratio H/z_0, or, an increase in windbreak height relative to the effective terrain roughness.

In regard to (ii) above, Plate [5] suggests a drag law of the form

$$C_{D*} = F_D/(\tfrac{1}{2}\rho u_*^2 H) = A \log (H/z_0) + B \qquad (1)$$

where A and B are constants

Equation (1) was proposed in analogy to a drag law derived by Good and Joubert [6] for impermeable barriers mounted in a smooth wall boundary layer. This equation is more relevant to the fully aerodynamically rough flows mostly found in nature, and implies that the smoother the terrain on which a windbreak of given height and permeability is erected, the greater will be the reduction in mean velocity in the leeward flow.

2.2 Influence of approach wind velocity profile and turbulence structure

It was not until the late 1950's that the importance of the turbulence structure in the approach flow was clearly recognised, and it is still common to find windbreak models tested in smooth wall boundary layers. It has been found that with increasing upstream terrain roughness and more turbulent approach flow, the smaller is the zone of reduced wind velocity downstream of the windbreak. Flow reattachment distances and drag coefficients for impermeable fences tested in different wind-tunnel flows illustrate this. Arie

and Rouse [7] tested barriers with symmetrical tail splitter plates in uniform flow and found a reattachment distance on the splitter plate of $17H$ (H = half barrier width) at Reynolds numbers, $\bar{U}_\infty H/\nu$, of about 10^5, where the flow pattern had become independent of Re. The corresponding drag coefficient C_D was approximately 1.4. Good and Joubert [6] tested fences in a smooth wall turbulent boundary layer and found reattachment distances of $13H$ to $14H$ and, for example $C_D = 1.28$ at $Re_H = 1.76 \times 10^5$. de Bray [8] tested fences in a partially simulated atmospheric boundary layer generated by a curved perforated metal screen, with and without additional floor roughness in the form of wooden blocks. Here reattachment distances of $11.6H$ and $11.2H$ were found for approach flow velocity profiles that were 1/7 and 1/4 power law respectively. The corresponding drag coefficients were 0.72 and 0.66 respectively.

With permeable fences also, less reduction in mean wind speed and lower drag coefficients can be expected with increasing approach flow turbulence (or velocity-profile power-law exponent). This is shown by results of de Bray [8] for fences of 50%, 55% and 70% permeability. Reports indicate that reattachment distances of $10H$ to $15H$ occur in the field. Kaiser [3] recognised the importance of approach-flow turbulence and attempted to quantify the dependence of windbreak performance on the upstream surface roughness. He postulated a 'wind reduction extension factor' to equate results from one test site to those measured over different terrain. Such factors should not be required in scaling up wind-tunnel test results if the model flow is correctly simulated.

A similarity analysis of the turbulent Navier—Stokes equations for the atmospheric boundary layer leads to flow modelling parameters, which, if held the same in both model and full-scale flow, should enable the wind-tunnel model to accurately predict full-scale performance. Assuming fully aerodynamically rough flow and geometric similarity of the two fences, then the four basic similarity parameters are,

$$z/z_0,\ \sqrt{\overline{u_0^2}}/\bar{U}_0,\ L_{u_x}{}_0/z_0 \text{ and } \bar{U}_0 z_0/K_{M_0}.$$

The first of these is a geometric scaling parameter, the second and third require similarity of profiles of turbulent intensity and integral scale respectively, and the fourth indicates that the shear-stress profiles and momentum-transfer processes in the model and full-scale flows should be similar. These modelling parameters imply similarity of the approach flow turbulence structure. More specifically, the spectral density $nS(n)/\overline{u^2}$ should be the same in model and full-scale flows at the same dimensionless frequency, $nH/\bar{U}$, and relative height, z/H. In an equilibrium rough wall boundary layer, Jensen's simple model law may suffice for similarity:

$$H_m/z_{0m} = H_a/z_{0a} \qquad (2)$$

This law is not adequate for the non-equilibrium boundary layer found at the model test position in most wind-tunnel simulations.

The modelling parameters above take cognisance of the fact that with increasing surface roughness the approach flow turbulence will be higher, and this causes a more rapid recovery of streamwise momentum in the leeward zone. Tests of flat plates in uniform flows of different turbulent intensities (Bearman [9]) indicate that eddies whose scale is of the order of the fence height are important in this mixing process.

Jensen's [10] results were the first clear demonstration in the field that increasing approach flow turbulence caused poorer mean wind reduction downstream of a windbreak. Baltaxe [11] and van Eimern et al. [1] also note the importance of the approach wind structure. The latter in their review cite reductions of windspeed of at least 20% for distances of $18H$—$27H$ downstream of windbreaks on level land in Denmark, but distances of only $7H$—$18H$ in the more mountainous terrain of Switzerland where the surface roughness tends to be much larger relative to windbreak height.

2.3 Influence of approach wind mean velocity

It is frequently assumed that bluff bodies, e.g., fences or buildings, erected in a turbulent wind, have leeward flow patterns independent of Reynolds number, Re_H. If H varies, this will only be true when the ratio H/z_0 remains constant. If the approach flow velocity $\overline{U}_\infty$, varies, leeward flow patterns may change depending on the upstream surface roughness. Both Jensen [10] and Kaiser [3] concluded that in fully aerodynamically rough neutrally stable flow, windbreak leeward flow patterns should be independent of approach flow velocity. This is suggested by eqn. (1) and is generally accepted today. In cases where a change in wind protection has accompanied a change in mean wind velocity, such as reviewed by Baltaxe [11] and van Eimern et al. [1], a change in atmospheric thermal stability has usually occurred.

Early wind-tunnel tests of model shelter fences were almost invariably carried out in the smooth floor boundary layer of an aeronautical wind tunnel (e.g., see Woodruff and Zingg, [13]). In such tests similarity of the Reynolds number $\overline{U}_H H/\nu$ was used as the modelling criterion. Because the importance of the wind's turbulence was not recognised, results from such tests were only a qualitative indication of full-scale windbreak performance.

2.4 The leeward flow field — influence of windbreak permeability

The pressure drop in the bleed flow as it passes through a windbreak is followed by pressure recovery in the flow downstream of the windbreak. With decreasing permeability the pressure drop across the windbreak increases. Plate [5] illustrates that with a less permeable barrier, the lower base pressure is accompanied by a stronger Coanda effect causing earlier reattachment of the displacement flow downstream of the barrier. When the windbreak permeability is low, stagnation occurs downstream in the bleed flow. The lower the permeability of the windbreak, the closer behind it lies the

stagnation point, and the mean flow pattern in this vicinity is poorly defined. However, with a solid fence there is a well defined recirculating eddy in the separation zone.

Most observations agree (e.g., van Eimern et al. [1]; Baltaxe [12]) that above a geometric permeability of 35%—50% a zone of stagnated flow and large-scale eddying (eddy scale of the order of the fence height) is no longer evident in the leeward flow. Such observations are supported by the analogous work of de Bray [14] and Valensi and Rebont [15] who tested bluff rectangular plates of various permeabilities in uniform flow. With windbreaks the upper limit of 50% permeability could be expected where the openings in the barrier are more sharp-edged.

The literature is generally vague concerning the relationship between mean velocity and turbulence in the leeward flow. Early work was mostly done with cup-counter anemometers with occasional visualisation of turbulence by means of tatter rags or rotating vanes. Effects of turbulence were often missed. For instance, van Eimern et al. [1] say: "Beneath the peak of the airflow is the zone of greatest wind reduction, the 'dead calm area' as Kreutz has called it". van Eimern et al. point out that more recent field reports show that zones of large mean velocity reduction are also zones of intense turbulence. This is verified by experimental results in Section 3 of this paper.

Available field and wind-tunnel results indicate that with increasing windbreak permeability there is a lesser reduction in mean velocity and lower turbulence intensity in the near wake, but a slower recovery to the upstream condition in the far wake. At the same time the mean velocity minimum, which occurs close to the ground, moves further downstream from the fence and lies at or just upstream of the zone of strongest turbulence. With a more permeable fence and consequently higher bleed flow velocity, there is less shear in the flow at the fence-top and thus weaker streamwise momentum transfer from the displacement flow back into the sheltered region.

Windbreak generated turbulence should ideally be of small scale and inten sity so as to decay rapidly. Data of Baines and Peterson [16] and Naudascher and Farell [17], obtained from wind-tunnel tests of screens, indicate that for a barrier of given geometric permeability, ϕ, the turbulence intensity and scale at a given location x/H downstream increases with the size of the elements in the barrier, i.e., with the coarseness of the permeability. As a general rule it is therefore desirable that a shelter fence should have fine rather than coarse openings in it.

Caborn [18] and van Eimern et al. [1] give good summaries of field windbreak performance. The latter summarise their review by saying: "the sheltered zone reaches up to about $30H$ in the lee and $5H$ to windward of the belt, but that for a wind reduction of 20% or more, only $20H$ should be reckoned". They reviewed reports where mean wind-speed reductions extending anywhere between $1H$ and $10H$ to windward and $8H$ to $60H$ to

leeward were found. Reconciling such variations requires information on the approach flow structure and wind measurement heights, z/H. More recent data for tree and hedge windbreaks are given by Sturrock [19] and for fence windbreaks by Hagen and Skidmore [20]. Data from these authors is used in Fig.4.

An optimum windbreak permeability of 35%—50% is often suggested [1, 18, 20]. This is based on best overall reduction in mean velocity given by an integral of $\bar{U}/\bar{U}_0$ over the distance of say $20H$ downstream, usually measured at a single height 1 to 2 m off the ground. However the optimum permeability appears to depend on the permeability configuration, the approach flow structure and the number of measurement heights in the leeward flow. For instance, at low H/z_0 ratio (probably less than 40) Schultz and Kelly [21] found an optimum permeability of 25% for a 1.22-m-high vertically slatted snow fence, measured at a height $z/H = 0.5$. Hagen and Skidmore [20], measuring at $z/H = 0.125$, found an optimum fence permeability of 40% based on the integral $\int_2^{20} \bar{U}/\bar{U}_0 \mathrm{d}\,(x/H)$. However their graphed data indicate that if the overall reduction in wind speed were evaluated over several heights using $\int_0^2 \int_2^{20} \bar{U}/\bar{U}_0 \mathrm{d}\,(x/H)\,\mathrm{d}\,(z/H)$, their 20% permeable fence would have been the optimum.

Typical field data [1, 10, 18—21, 23, 25] indicate that an effective windbreak should give a mean velocity reduction of 50% up to $10H$ downstream, 20% up to $20H$ downstream and a maximum reduction of 70%—80% $1H$ to $5H$ downstream, these values measured at $z/H = 0.5$. Effects of the windbreak on the flow may still be noticeable $60H$ to $100H$ downstream. The vagueness in many reports of field work shows a need to specify accurately approach flow boundary layer structure, geometric permeability of the windbreak and measuring instrument heights.

3. Wind tunnel tests of model shelter fences

3.1 Experimental procedure

The model fences were located 9.15 m downstream from the entrance to the wind-tunnel working section, immersed in a boundary layer 0.9 m deep. Profiles of mean velocity and u component turbulence intensity for this model atmospheric flow are shown in Fig.2. Energy spectra for the u velocity component in the approach flow at $z = 50$ mm, 150 mm and 600 mm are shown in Fig.3. More complete data for the turbulence structure of the flow are given by Raine [2].

Fences of permeability 0%, 20%, 34%, 50% and 59% were tested, and various distributions of permeability used. Discussion in this paper is restricted to results obtained from four representative fences:

0% permeable — 16-gauge aluminium alloy,
20% permeable — horizontal evenly spaced wood slats, $B/H = 0.064$.
24% permeable — uniformly punched 20-gauge steel sheet, $D/H = 0.08$,
50% permeable — horizontal evenly spaced wood slats, $B/H = 0.064$.

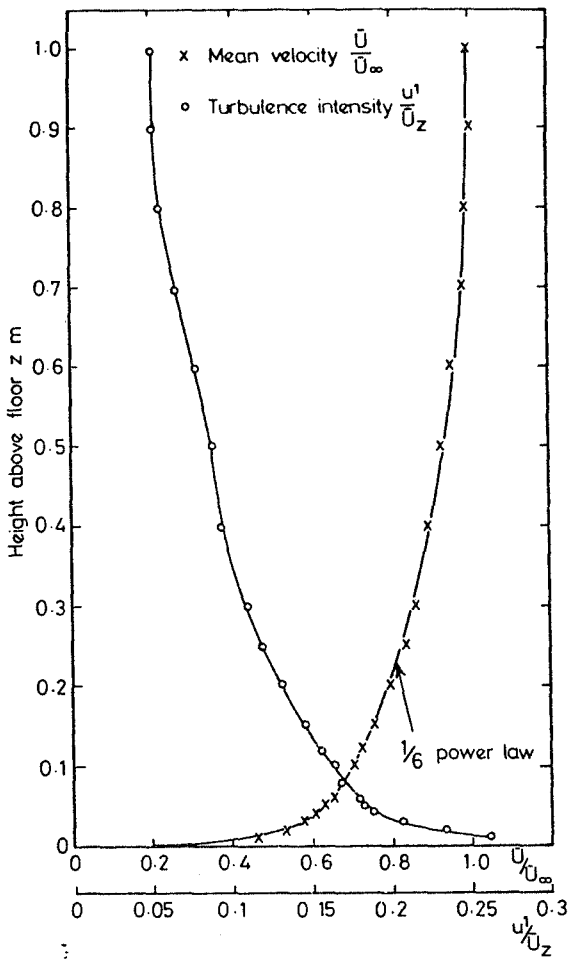

Fig.2. Approach flow mean velocity and turbulence intensity profiles.

For the main tests a fence height of 50 mm was used, causing only 4% blockage of the 1.22 m X 1.22 m cross-section of the wind tunnel. Initially scale-effect tests were carried out with fences of 25 mm, 50 mm and 100 mm heights. Surface roughness downstream of the fences was Torro baseboard, similar to Lego.

Flow measurements were restricted to mean velocity, $\overline{U}$, velocity fluctuations, u, and u component energy spectra. Flow measurements were made with two linearised DISA 55DOO hot-wire anemometer sets, using 55 F31 and 55 F25 miniature single-wire probes with the wire set horizontal and the mean flow perpendicular to the wire. The hot-wire signals were also fed from the anemometers to a Bruel and Kjaer Type 2114 1/3 octave bandwidth spectrometer and Type 2305 level recorder for spectral analysis. Analysis of the effects of mean flow inclination and large turbulence intensities on the

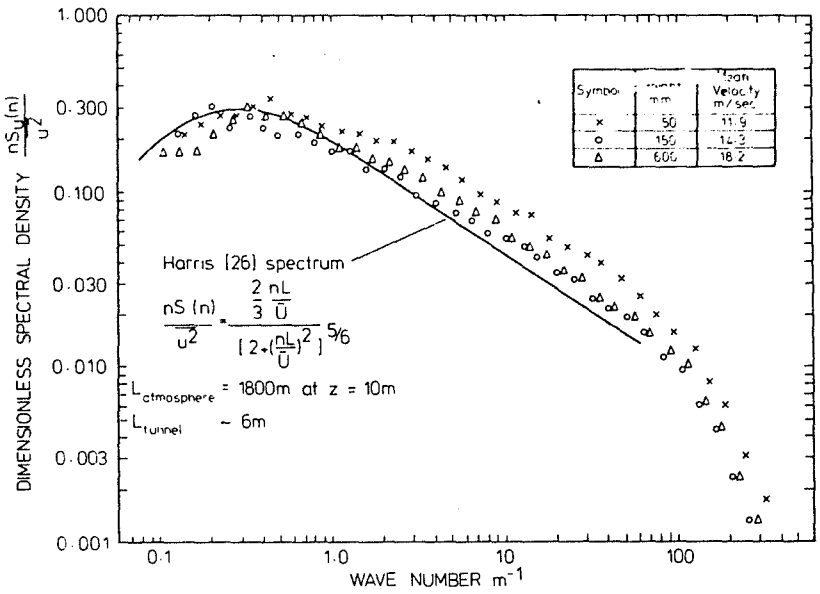

Fig. 3. Energy spectrum for the u velocity component in approach flow.

linearised constant-temperature hot-wire signal in the fence leeward flow indicated possible errors on $\overline{U}$ and $u'/\overline{U}$ of about ± 1% at $u'/\overline{U} = 0.2$ and ± 5% at $u'/\overline{U} = 0.4$. The need to know higher than second-order correlations of the turbulent velocity components at high turbulence intensity rendered the error analysis very approximate. However, it was considered that the hot-wire anemometer would give acceptable quantitative information for engineering applications. Hot-wire traverses were made to a distance of $45H$ downstream of each fence and to a height of $4H$. After checking lateral uniformity, traverses were restricted to a point just off the tunnel centreline.

The linear scale of the simulated atmospheric flow was about 1:300 based on matching the wind-tunnel u velocity component spectra with the model atmospheric spectrum of Harris [26]. The value of z_0 estimated from the approach flow mean velocity profile was consistent with a 1:300 model scale, and at the windbreak position H/z_0 was about 100.

The preliminary scale effect tests showed a consistent trend for greater mean velocity reduction and higher turbulence intensity at any leeward point $(x/H, z/H)$ as fence height increased. For example, with both solid and 50% permeable fences, values of relative velocity, $\overline{U}/\overline{U}_0$, were up to 30% lower when H = 100 mm than when H = 25 mm. This trend with increasing H/z_0 bears out comments made in section 2.1. It also emphasises that the model-fence height should be chosen in accordance with the requirement for scaling the approach flow turbulence spectrum $nS(n)/u^2$ versus $nH/\overline{U}$ pointed out in section 2.2.

3.2 Results and discussion

The $\bar{U}/\bar{U}_0$ isotachs, plotted in Fig.4 for each of the four fences, exhibit a generally greater mean velocity reduction with decreasing fence permeability. There is an accompanying increase in the maximum displacement flow velocity, and the velocity minimum moves closer to the fence. Secondary velocity minima occur at $x/H = 0+$ and $z/H = 0.7$ with the 34% and 50% permeable fences. With the solid fence the downstream flow reattachment point was at $x/H = 9$. Wind-reduction performance of the different fences was compared by evaluating the integral (for each fence)

$$\text{'Total Velocity'} = \int_0^{1.5} \int_0^{45} \bar{U}/\bar{U}_0 \mathrm{d}(x/H)\mathrm{d}(z/H) \qquad (3)$$

On this basis the best overall wind-velocity reduction (lowest 'Total Velocity') was given by the 20% permeable fence, and the order of merit for the different fence permeabilities was 20%, 0%, 34%, 50%. The isotachs of Fig.4 show good similarity to field results of Hagen and Skidmore [20]. In Fig.5 comparison of horizontal mean velocity profiles with earlier work [1, 8, 10, 12, 13, 19–25] is made at the height $z/H = 0.5$. This height was chosen to suit availability of data from other reports, and the above order of merit for the fence permeabilities was preserved with eqn. (3) evaluated at $z/H = 0.5$ only.

In Fig.5 there is considerable scatter between different test results owing to differences in terrain, atmospheric stability and thus in effective H/z_0 ratio. With the solid fence, for instance, at $x/H = 12$ $\bar{U}/\bar{U}_0$ varies between about 0.2 and 0.6. There is, however, a clear trend for greater mean wind reduction with increasing H/z_0, and the present test results agree well with field results where a similar H/z_0 value prevails. This comparison of field and wind-tunnel windbreak performance would be better referred to the approach flow turbulence spectrum content in each case. However, field-test results usually give a description of only the surrounding terrain and perhaps the approach flow mean velocity profile; hence H/z_0 makes a convenient if less precise scaling parameter.

Graphs of $u'/\bar{U}$ 'isoturbs', or constant-turbulent-intensity contours are shown in Fig.6. Lower turbulent intensity at any location (x/H, z/H) is generally found as fence permeability increases. Compare for instance the relative position of the 0.4 or 0.5 isoturb. Comparison of Fig.6 with Fig.4 clearly shows that regions of high turbulent intensity are regions of low mean velocity, also that respective turbulent intensity maxima close to the ground lie $1H$ to $2H$ downstream of mean velocity minima. For a given value of $\bar{U}/\bar{U}_0$, $u'/\bar{U}$ tends slightly higher with less permeable fences, apparently due to stronger shear in the flow at the fence top. To examine more closely the relationship between mean velocity and turbulent fluctuations in the leeward flow, the u' fluctuations were plotted as $u'/\bar{U}_H$ isoturbs in Fig.7. This shows that at any downstream point (x/H, z/H) the RMS fluctuation, u', varies much less with permeability than does mean velocity, $\bar{U}$, indicating that higher values of $u'/\bar{U}$ behind denser fences are due more to a large reduction in $\bar{U}$ than to higher u' levels.

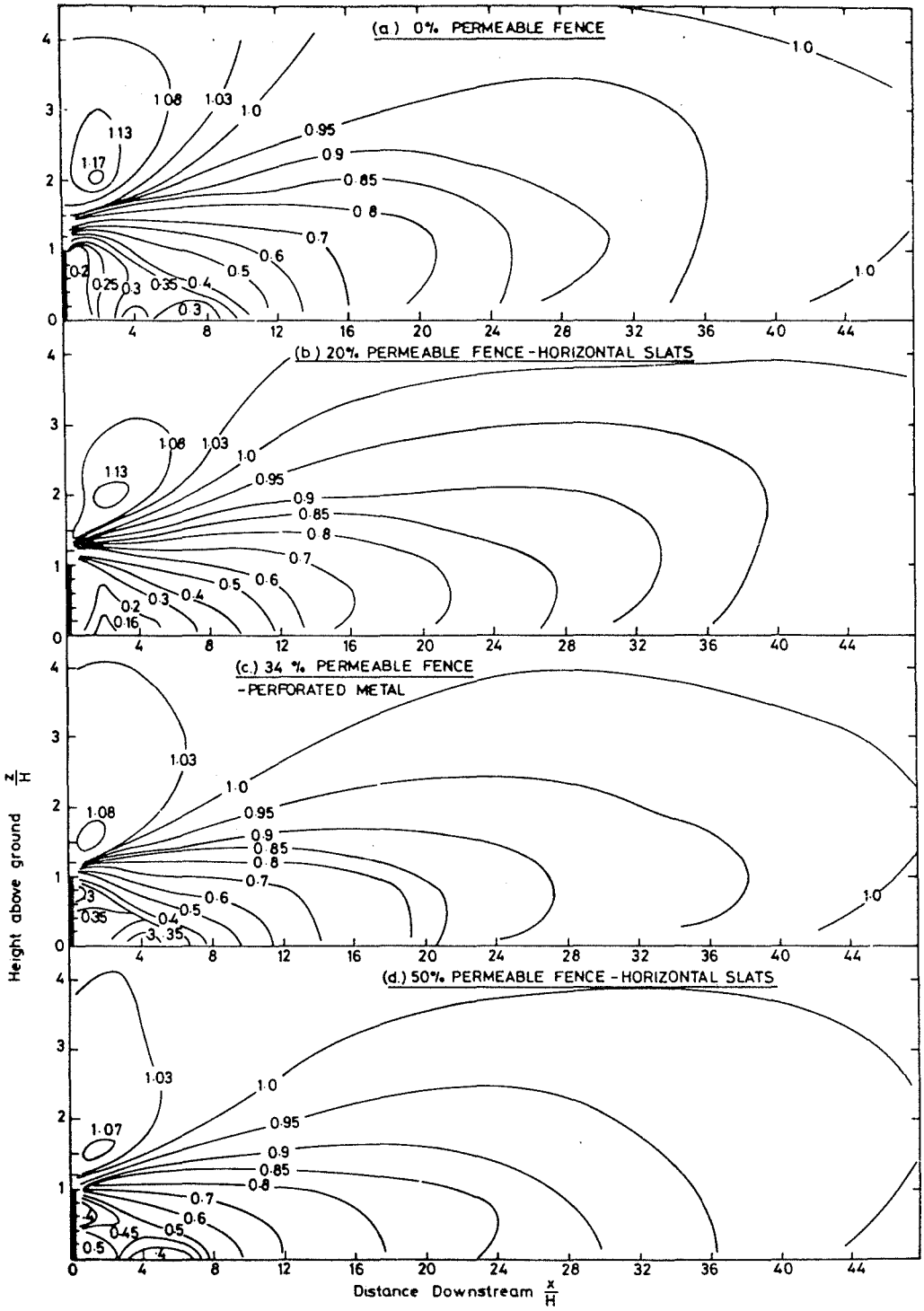

Fig.4. $\bar{U}/\bar{U}_0$ isotachs downstream of fences of different permeability. $\bar{U}_H$ = 11.34 m/sec.

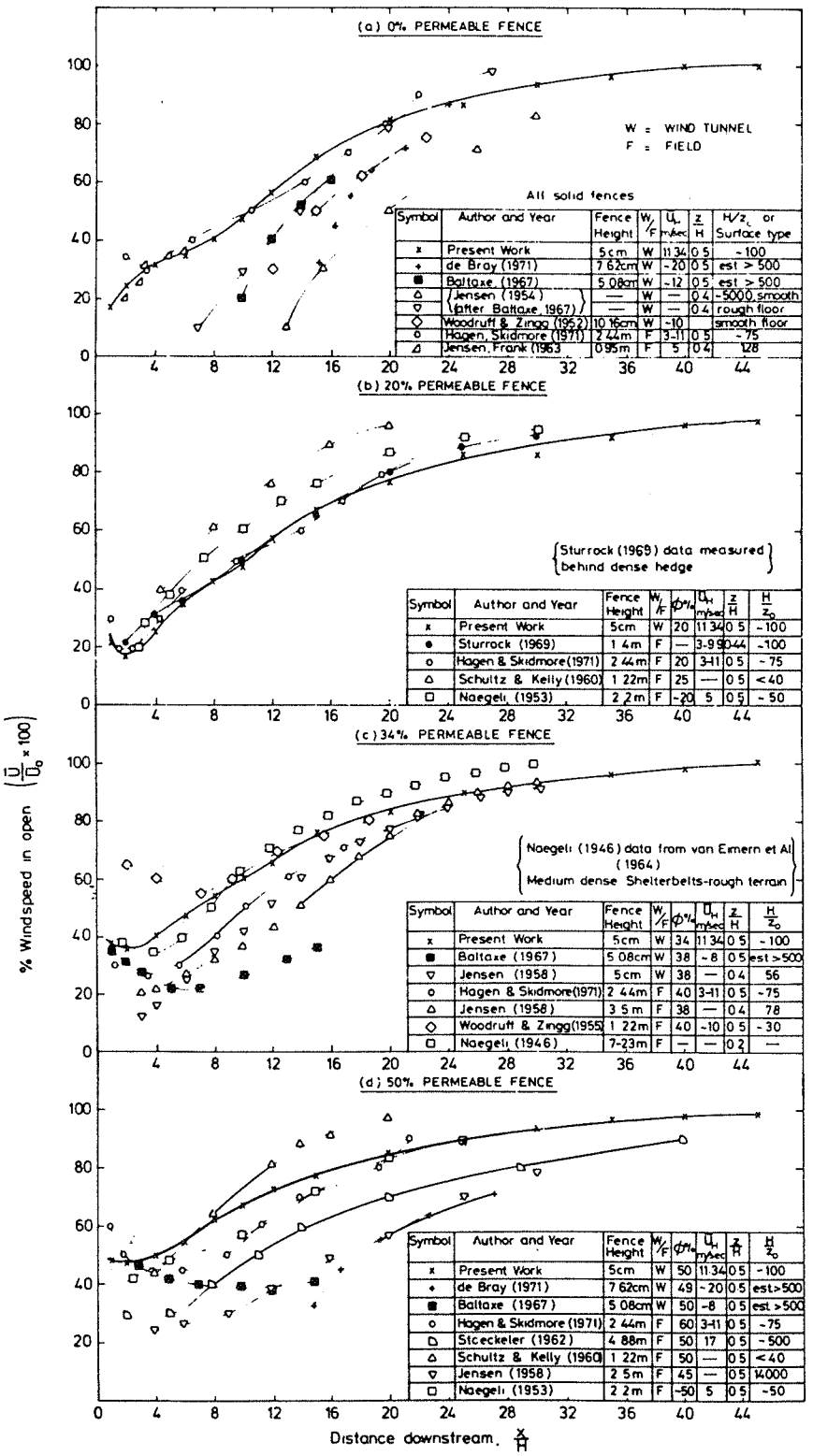

Fig.5. Horizontal mean flow velocity profiles downstream of model fences of different permeability — comparison with previous results.

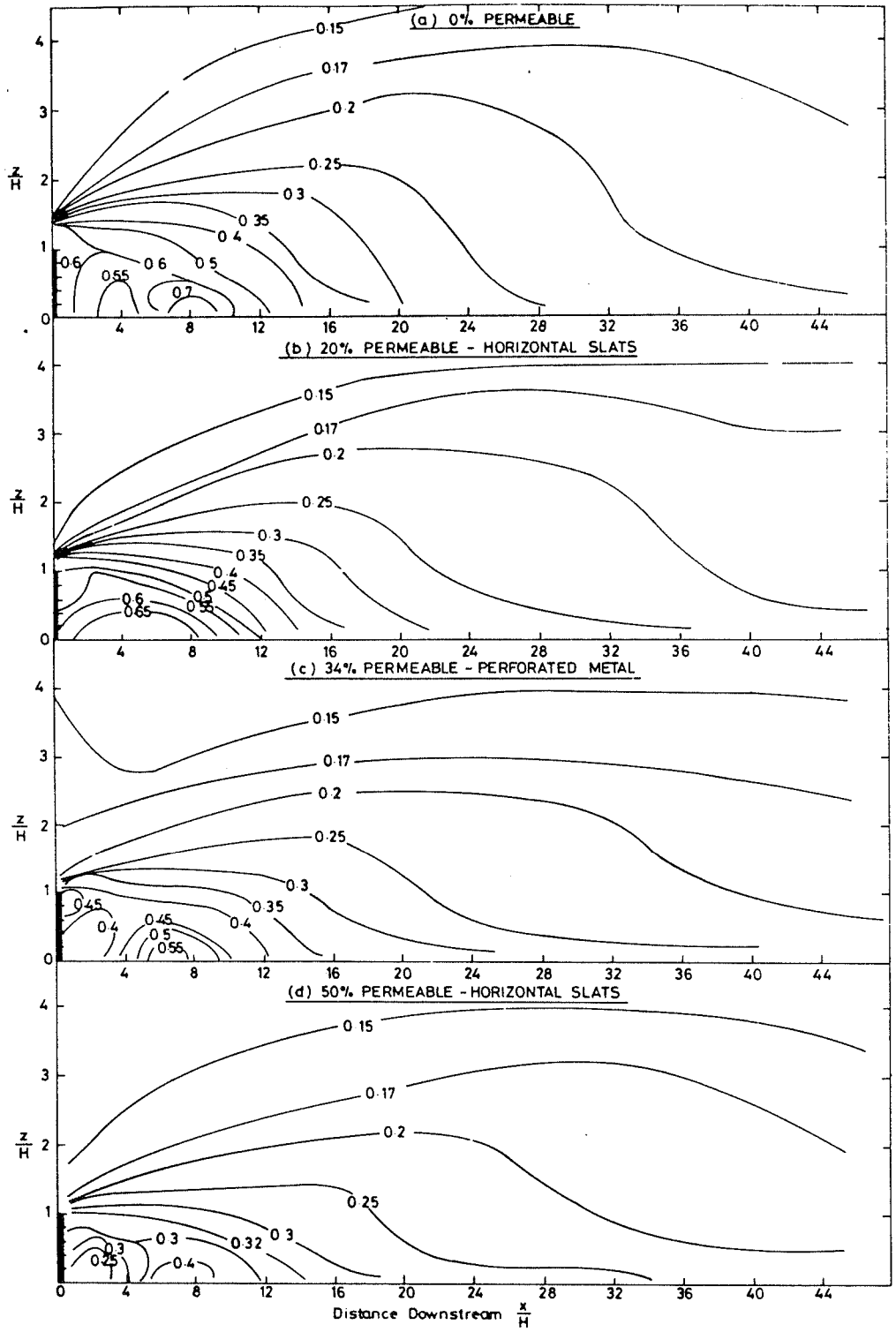

Fig. 6. $u'/\overline{U}$ isoturbs downstream of fences of different permeability. $\overline{U}_H$ = 11.34 m/sec.

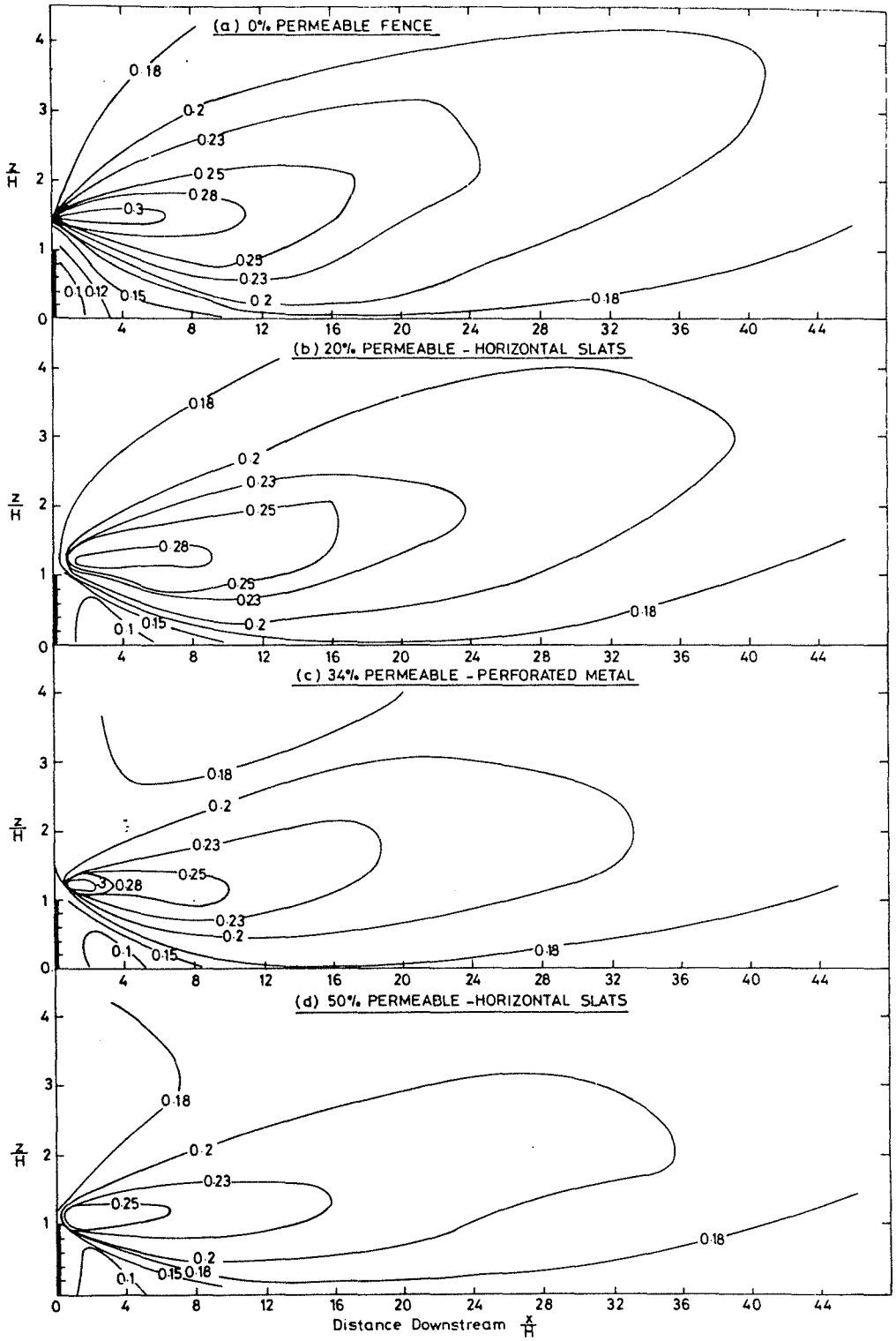

Fig.7. $u'/\overline{U}_H$ isoturbs downstream of 50-mm fences of different permeability, $\overline{U}_H$ = 11.34 m/sec.

Since $\bar{U}_H$ is constant, Fig.7 is a dimensionless plot of absolute RMS fluctuation levels and shows that the maximum value of u' occurs not close to the ground as with $u'/\bar{U}$ but just above and to leeward of the top of the fence. Thus the high shear initiated at the fencetop is the dominant source of turbulent velocity fluctuations in the leeward flow, even with the most permeable fence. This turbulence diffuses vertically as it is convected downstream by the displacement flow and enhances streamwise momentum transfer down into the sheltered zone. In the approach flow, the value of $u'/\bar{U}_H$ was approximately 0.2 up to $z/H = 2$. Fig.7 shows, therefore, that over a significant part of the leeward flow field below $z/H = 1$, the fence has caused a reduction in RMS velocity fluctuation level. This is particularly noticeable close behind the fence, where there is a triangular 'quiet' zone bounded by the fence, the ground, and the line joining the top of the fence to the ground at $x/H = 8.0$. In this zone u' determined by the bleed flow structure and thus by the fence permeability, is low so that $u'/\bar{U}_H$ is 0.1 to 0.12. The turbulence intensity, $u'/\bar{U}$, is nevertheless high because of the low mean velocity. The bleed flow begins to experience the displacement flow turbulence approximately along the line joining the top of the fence to the ground at $x/H = 8.0$. Near the ground $u'/\bar{U}$ maxima appear to occur along this line. Outside the 'quiet' zone the turbulence structure is dominated by the fluctuations of much greater magnitude diffusing downward from the fence-top turbulence source. Far downstream of the fence the approach flow turbulence intensity levels should be regained.

Interpreting the above results, the leeward flow is seen as regions dominated respectively by the bleed flow and by the displacement flow. The bleed flow reaches a velocity minimum, and the turbulence intensity an apparent maximum, in the intermittent flow zone at the boundary of the 'reattaching' displacement flow.

The relationship between turbulence intensity and mean velocity was further examined by plotting $u'/\bar{U}$ against $\bar{U}/\bar{U}_0$ for each fence and each leeward measurement point. It was found that for all the fences, outside the previously defined 'quiet' zone and below $z/H = 1.2$, $u'/\bar{U}$ was given to within ± 10% by the equation

$$u'/\bar{U} = \exp(-1.67\ \bar{U}/\bar{U}_0) + 0.1\ \{1 - (\bar{U}/\bar{U}_0)\} \qquad (4)$$

Results are plotted, for example, in Fig.8 for $z/H = 0.4$ and 0.6. The points lying outside the ±10% limits of eqn. (4) lie in the 'quiet' zone. Here the less well defined relationship between u' and $\bar{U}$ is given to within ±13% by the equation

$$u'/\bar{U} = 0.9 - 1.6\ \bar{U}/\bar{U}_H \qquad (5)$$

Equations such as 4 and 5 may be used to predict leeward turbulence intensity from known leeward mean velocity data. The −1.67 index and 0.1 coefficient in eqn. (4) will tend to vary with approach flow turbulent intensity.

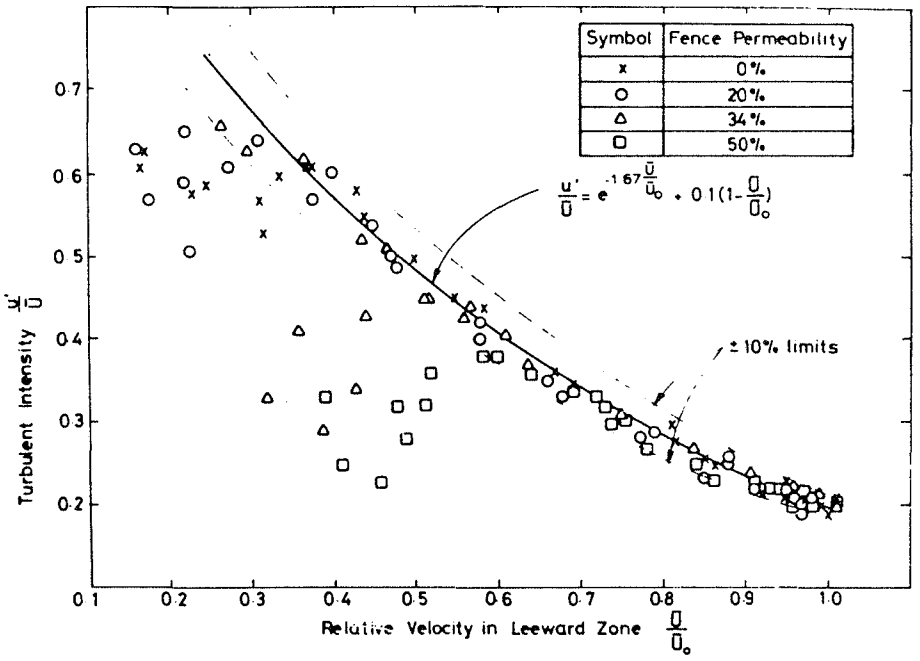

Fig.8. Graph of $u'/\overline{U}$ vs. $\overline{U}/\overline{U}_0$ at $z/H = 0.4$ and 0.6 — all four fences.

Energy spectra for the u velocity component are shown in Fig.9. Figure 7 indicates that close to the fence ($x/H = 2$, $z/H = 0.6$) the spectrum should be dominated by the relatively-small-scale turbulence generated by the permeability elements of the fence, but further downstream ($x/H = 6$ and 15) the spectrum should be dominated by the displacement flow and fence-top generated turbulence. In Fig.9 it is seen that this does occur. Close to the fence ($x/H = 2$) the high-frequency turbulence shed by the fence elements controls the spectrum shape, the dimensionless peak frequency being in every case higher than in the approach flow, and this peak frequency increasing with fence permeability. With the solid fence, this frequency is determined by the approach flow velocity, $\overline{U}_H$, and the fence height, H. At $x/H = 6$ the influence of the larger-scale and more-intense fluctuations in the displacement flow causes a regression towards the common approach flow spectrum shape and generally towards a lower spectral peak frequency. At $x/H = 6$ the solid fence shows its highest peak frequency, a feature also noted by Hagen and Skidmore [20]. At $x/H = 15$ the spectra have largely recovered the approach flow shape and a common peak frequency which is still a factor of 2 to 3 higher than in the approach flow. At this point the flow has more or less 'forgotten' the influence of the fence permeability. Spectral peak frequency data summarised in Table 1 (which includes data from additional fences) bear out the comments made above. In both Fig.9 and Table 1, the more permeable fences appear to recover the upstream

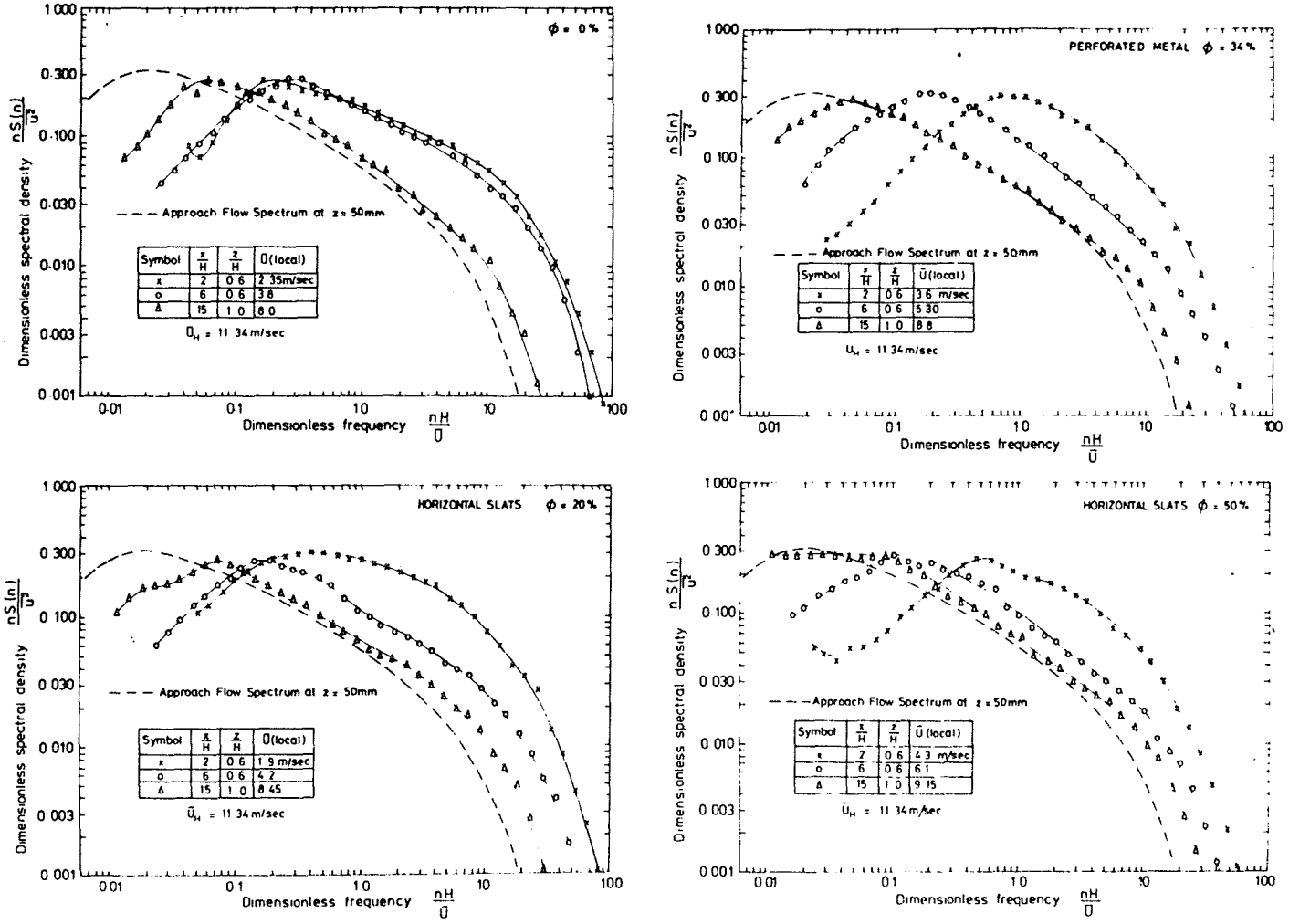

Fig.9. Energy spectra downstream of fences of different permeability.

TABLE 1

Spectral peak frequencies for the u velocity component at locations (x/H, z/H) downstream of different 50-mm-high fences

FENCE TYPE	Φ %	$\frac{x}{H}=2$, $\frac{z}{H}=0.6$			$\frac{x}{H}=6$, $\frac{z}{H}=0.6$			$\frac{x}{H}=15$, $\frac{z}{H}=1$		
		n_p Hz	$\left(\frac{nH}{\bar{U}}\right)_p$	$\frac{\bar{U}}{\bar{U}_o}$	n_p Hz	$\left(\frac{nH}{\bar{U}}\right)_p$	$\frac{\bar{U}}{\bar{U}_o}$	n_p Hz	$\left(\frac{nH}{\bar{U}}\right)_p$	$\frac{\bar{U}}{\bar{U}_o}$
Aluminium	0	8	0.17	0.23	22.5	0.3	0.37	-10	0.062	0.7
Horizontal Wood Slats	20	16	0.41	0.18	14.3	0.17	0.38	12.5	0.074	0.74
Vertical Wood Slats	20	50	1.7	0.14	14.3	0.23	0.33	12.5	0.076	0.71
Perforated 20G Steel	34	50	0.69	0.32	18	0.17	0.51	8	0.046	0.71
Torro Blocks	34	40	0.69	0.27	18	0.16	0.48	8	0.044	0.79
Horizontal Wood Slats	50	40	0.46	0.41	14.3	0.10	0.58	-8	0.044	0.8
Vertical Wood Slats	55	100	0.95	0.53	16	0.13	0.62	8	0.043	0.85
Wood Lattice Work	59	160	1.41	0.54	16	0.12	0.65	10	0.049	0.88
Average Peak Frequency		58	0.81		16.7	0.17		9.63	0.055	
Standard Deviation, σ		49.6	0.52		2.98	0.06		2.0	0.014	
σ - (Average)		0.86	0.64		0.18	0.35		0.21	0.26	
Approach Flow Values*		6.3	0.024		6.3	0.024		6.3	0.024	

* at z = 50mm

form and dimensionless peak frequency more rapidly with downstream distance than does the solid fence. This is perhaps to be expected. The solid fence can be visualized creating a greater disturbance to the approach flow and contributing a more permanent small eddy field to the larger-scale upwind turbulence.

The observer behind a windbreak in the field usually reports 'high turbulence' in regions of low mean velocity, and thus appears to notice the turbulence intensity, $u'/\bar{U}$ rather than the velocity fluctuations, u. However, the definition of an 'effective velocity', in which the mean velocity at any point must be weighted to allow for the annoying or damaging effect of the turbulence intensity, has not been established. In the results presented, $\bar{U}/\bar{U}_0$ required weighing very heavily, e.g., by forming the sum $(\bar{U}/\bar{U}_0 + u'/\bar{U})$ in order to change the heirarchy of wind-protection performance given by eqn. (3). Generally it is desirable to obtain a large mean wind reduction without raising turbulent fluctuations to a level where they are damaging. Criteria are needed for the importance of shelter-fence leeward turbulence in agriculture, industrial and commercial areas. In recreation areas, subjective human-comfort tests carried out with people at leisure behind fences of various permeabilities may help define an effective wind-shelter velocity.

Optimum mean wind reduction appears to be obtained with a 20%—30% permeable fence. However, for little sacrifice in maximum wind reduction, the builder with a fixed quantity of materials at his disposal may do better

to construct a fence, say 3 m high and 50% permeable, rather than 2 m high and 25% permeable. The higher fence would extend the height and fetch of the leeward sheltered zone, in particular far downstream, as shown in Fig.10. Improved shelter, in the form of lower turbulence intensity for a given mean velocity reduction, may be obtainable by reducing the strong shear in the flow at the fence top. In practice this suggests a fence with permeability increasing from 0% at the base to 100% at the top.

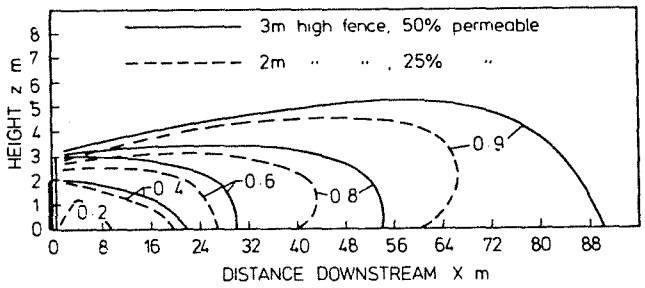

Fig.10. Example of $\overline{U}/\overline{U}_0$ isotachs likely to be obtained downstream of 2 fences of similar material cost. Protection given by 3-m fence is substantially better far downstream.

4. Conclusions

Tests of fences of four permeabilities have shown that model shelter fences tested in a wind-tunnel flow may accurately predict full-scale performance provided the atmospheric wind is modelled. Profiles of mean velocity, Reynolds stress, turbulence intensity, spectra and integral scale should be correctly scaled.

Measurements of turbulence intensity and spectra for the u velocity component in the fence leeward flows have given a clearer picture of the respective zones of influence of the bleed flow and the displacement flow, and show the rapid domination of the leeward turbulence field by the turbulence diffusing into the sheltered zone in the 'reattaching' displacement flow. Equations have been given relating turbulence intensity and relative mean velocity in:

(i) the 'quiet' zone dominated by the bleed flow
(ii) the more leeward part of the sheltered zone dominated by the displacement flow.

Before such equations can be usefully applied, quantitative field tests are needed to determine the relative importance of leeward turbulence levels and mean velocity reduction.

The experimental results have confirmed that a windbreak of low to medium permeability gives better overall mean wind reduction than a solid windbreak, and for the same price a higher more permeable fence can give better overall protection.

5. Acknowledgement

The authors gratefully acknowledge the financial support of the New Zealand University Grants Committee, who assisted with funds for the construction of the atmospheric boundary layer wind tunnel.

List of symbols

x, $\bar{U}$, u	streamwise direction, mean velocity and fluctuating velocity respectively
u'	root mean square of the fluctuating u velocity component $\sqrt{\overline{u^2}}$
y, $\bar{V}$, v	lateral direction, mean velocity and fluctuating velocity respectively
z, $\bar{W}$, w	vertical direction, mean velocity and fluctuating velocity respectively
z_0	roughness length of the upstream terrain
F_D	drag force
C_D	drag coefficient referred to mean velocity, $\bar{U}_\infty$, at outside of boundary layer
C_{D*}	drag coefficient based on friction velocity, $u* = \tau_0/\rho$, in the approach flow velocity profile
τ_0	surface shear stress
ρ	density of air
ν	kinematic viscosity of air
H	fence height
0	subscript which in Section 2.2 indicates a quantity evaluated at a reference height which is a constant multiple of the roughness length in both model and full-scale flows
L_{u_x}	integral scale of turbulence of the u velocity component in the streamwise direction
K_M	eddy viscosity
m, a	subscripts referring to model and full scale flow respectively
ϕ	geometric permeability of fence, = (open area)/(total area)
$\bar{U}_0$	(other than in 2.2) approach flow mean velocity at same height as measurement height in leeward flow
$\bar{U}_H$	approach flow mean velocity at $z = H$
B	width of fence slat
D	diameter of hole in fence
Re	Reynolds number: $Re_H = \bar{U}_H H/\nu$

References

1 J. van Eimern, R. Karschon, L.A. Razumova and G.W. Robertson, Windbreaks and shelterbelts, World Met. Org. Tech. Note No. 59, 1964.

2 J.K. Raine, Simulation of a neutrally stable rural atmospheric boundary layer in a wind-tunnel, Proc. 5th Australasian Conf. on Hydraulics and Fluid Mech., Christchurch, New Zealand, Dec. 1974.
3 H. Kaiser, Die Stromung an Windschutzstreifen (The airflow through shelterbelts), Berichte Deutscher Wetterdienstes, 7, No. 53, 1959.
4 I. Seginer and R. Sagi, Drag on a windbreak in two-dimensional flow, Agric. Meteorol., 9 (1972—73) 323—333.
5 E.J. Plate, The aerodynamics of shelterbelts, Agric. Meteorol., 8 (1971).
6 M.C. Good and P.N. Joubert, The form drag of two-dimensional bluff plates immersed in turbulent boudary layers, J. Fluid Mech., 31 (3) (1968) 547—582.
7 M. Arie and H. Rouse, Experiments on two-dimensional flow over a normal wall, J. Fluid Mech., 1 (2) (1956).
8 B.G. de Bray, Protection by fences, Proc. Seminar on Wind Effects on Buildings and Structures, Univ. of Auckland, New Zealand, May, 1971.
9 P.W. Bearman, Some recent measurements of the flow around bluff bodies in smooth and turbulent streams, Paper presented at a Symposium on External Flows, Univ. of Bristol, July, 1972.
10 M. Jensen, The model law for phenomena in the natural wind, Ingenioren, Int. Edn., 2 (1958) 151.
11 R. Baltaxe, The Vertical profile of wind speed near the ground as a criterion of turbulence in relation to shelter, Proc. 13th Congr. Int. Union For. Res. Organ., Vol. 2, 1961.
12 R. Baltaxe, Air flow patterns in the lee of model windbreaks, Arch. Meteorol. Geophys. Bioklimatol., Ser. B, Band 15, Heft 3 (1967).
13 N.P. Woodruff and A.W. Zingg, Wind tunnel studies of fundamental problems related to windbreaks, U.S. Dept. Agric. Soil Conservation Service in co-operation with the Kansas Agric. Expt. Stat., SCS-TP-112, Aug. 1952.
14 B.G. de Bray, Low speed wind tunnel tests on perforated square flat plates normal to the airstream: Drag and Velocity Fluctuation Measurements, R.A.E. Tech. Note No. Aero 2475, Oct. 1956.
15 J. Valensi and J. Rebont, Aerodynamics of perforated walls. Application to wind protection [illegible] project: Study of the functioning of such screens, Paper 27, AGARD Fluid Dynamics Panel Specialists Meeting on the Aerodynamics of Atmospheric Shear Flow, Munich, Sept. 1969.
16 W.D. Baines and E.G. Peterson, An investigation of flow through screens, Trans. ASME (July, 1951).
17 E. Naudascher and C. Farell, Unified analysis of grid turbulence, Proc. ASCE (April, 1970).
18 J.M. Caborn, Shelterbelts and microclimate, Forestry Comm. Bull. No. 29, Edinburgh HMSO, 1957.
19 J.W. Sturrock, Aerodynamic studies of shelterbelts in New Zealand, 1: Low to medium height shelterbelts in mid-Canterbury, N.Z. J. Sci., 12 (4) (1969) 754—776; 2: Medium height to tall shelterbelts in mid-Canterbury, N.Z. J. Sci., 15 (2) (1972) 113—140.
20 L.J. Hagen and E.L. Skidmore, Turbulent velocity fluctuations and vertical flow as affected by windbreak porosity, Trans. ASAE (1971) 634—637.
21 H.B. Schultz and C.F. Kelly, Studies on wind protection efficiency of slatted fence windbreaks, Calif. Agric., 14 (4) (1960) 3, 11.
22 M. Jensen and N. Franck, Model scale tests, Part 1, The Danish Technical Press, Copenhagen, 1963.
23 W. Naegeli, Research on wind conditions in the vicinity of reed screens, Mitt. Schweiz. Anstalt. Forstl. Versuchswesen, Zurich, 29 (2) (1953).
24 N.P. Woodruff and A.W. Zingg, A comparative analysis of wind tunnel and atmospheric air flow patterns about single and successive barriers, Trans. Am. Geophys. Union, 36 (2) (1955).

25 J.H. Stoeckeler, Shelterbelt influence on great plains field environment and crops, U.S. Dept. Agric. Prod. Res. Rep. No. 62, 1962.
26 R.I. Harris, Measurements of wind structure at heights up to 598 ft above ground level, Paper 1, Proc. of Symp. on wind effects on buildings and structures, Loughborough Univ. of Technol., April, 1968.